Temporally resolved interactions between antigen-stimulated IgE receptors and Lyn kinase on living cells

Daniel R. Larson,[1] Julie A. Gosse,[2] David A. Holowka,[2] Barbara A. Baird,[2] and Watt W. Webb[1]

[1]School of Applied and Engineering Physics, and [2]Department of Chemistry and Chemical Biology, Cornell University, Ithaca, NY 14853

Upon cross-linking by antigen, the high affinity receptor for immunoglobulin E (IgE), FcεRI, is phosphorylated by the Src family tyrosine kinase Lyn to initiate mast cell signaling, leading to degranulation. Using fluorescence correlation spectroscopy (FCS), we observe stimulation-dependent associations between fluorescently labeled IgE-FcεRI and Lyn-EGFP on individual cells. We also simultaneously measure temporal variations in the lateral diffusion of these proteins. Antigen-stimulated interactions between these proteins detected subsequent to the initiation of receptor phosphorylation exhibit time-dependent changes, suggesting multiple associations between FcεRI and Lyn-EGFP. During this period, we also observe a persistent decrease in Lyn-EGFP lateral diffusion that is dependent on Src family kinase activity. These stimulated interactions are not observed between FcεRI and a chimeric EGFP that contains only the membrane-targeting sequence from Lyn. Our results reveal real-time interactions between Lyn and cross-linked FcεRI implicated in downstream signaling events. They demonstrate the capacity of FCS cross-correlation analysis to investigate the mechanism of signaling-dependent protein–protein interactions in intact, living cells.

Introduction

The IgE receptor FcεRI is a member of the multichain immune recognition receptor family and contains the IgE-binding subunit α and three immunoreceptor tyrosine-based activation motif (ITAM)–containing subunits, β and disulfide-linked γ_2 (Blank et al., 1989; Kinet, 1999). Cross-linking of IgE receptor complexes by multivalent antigen initiates ITAM phosphorylation in the cytoplasmic segments of FcεRI β and γ_2 by Lyn tyrosine kinase, resulting in the recruitment and activation of the tyrosine kinase Syk and the initiation of a downstream signaling cascade that leads to the cellular degranulation underlying allergic and inflammatory responses (Siraganian, 2003). Many studies have contributed to our understanding of the cooperative interactions between proteins and lipids involved in this process of signal initiation by FcεRI (Rivera et al., 2002; Holowka et al., 2005). In the resting state, FcεRI is almost randomly distributed at ∼100 molecules per square micrometer, and most of it is diffusively mobile in the plasma membrane. After cross-linking with multivalent antigen, the receptor forms puncta on the cell surface that are visible at the level of light microscopy, and a substantial fraction of the receptors are observed to be relatively immobile in photobleaching recovery experiments (Menon et al., 1986; Holowka and Baird, 1996). However, little is known about the dynamic behavior of intracellular signaling molecules such as Lyn and how these molecules interact with FcεRI and the plasma membrane during signal initiation. Lyn can interact with FcεRI or other proteins in an enzyme–substrate complex or via its SH2 or SH3 binding domains. Lyn also associates with the plasma membrane via a pair of saturated acyl chains at its NH_2 terminus (Xu et al., 2005). Real-time dynamics of these interactions at the plasma membrane have not been previously reported.

We approached this problem by directly monitoring the interactions between Lyn, FcεRI, and other plasma membrane–associated components (Fig. 1 A) using two-photon excitation fluorescence correlation spectroscopy (FCS; Webb, 2001). In this approach, a small diffraction-limited focal volume (∼0.1 μm^3 with a cross-sectional area ∼0.1 μm^2 on the membrane; Fig. 1 B, red oval intersecting cell membrane) is created by focusing a laser through an objective lens. Because of the nonlinear absorption of photons (two-photon excitation is

D.R. Larson and J.A. Gosse contributed equally to this paper.

Correspondence to Barbara A. Baird: bab13@cornell.edu; or Watt W. Webb: www2@cornell.edu

D.R. Larson's present address is Dept. of Anatomy and Structural Biology, Albert Einstein College of Medicine, Bronx, NY 10461.

Abbreviations used in this paper: FCS, fluorescence correlation spectroscopy; huIgE, human IgE; ITAM, immunoreceptor tyrosine-based activation motif; moIgE, mouse monoclonal DNP-specific IgE; RBL, rat basophilic leukemia.

The Journal of Cell Biology, Vol. 171, No. 3, November 7, 2005 527–536
http://www.jcb.org/cgi/doi/10.1083/jcb.200503110

proportional to I^2, where I = intensity of the laser), light is absorbed and fluorescence is emitted only in the vicinity of the focus of the lens, yielding a well defined optical focal volume (Denk et al., 1990). Diffusion of molecules into and out of this focal volume leads to characteristic fluctuations in fluorescence, which in turn can be used to determine dynamic quantities such as diffusion coefficients and reaction kinetics (Magde et al., 1972). If two distinguishable fluorescent species are present, one can analyze correlations between these molecular species indicative of codiffusion and association (Heinze et al., 2000). This phenomenon is illustrated in Fig. 1 C. Cross-correlation is independent of nanoscopic distance and relative orientation between fluorophores, in contrast to an alternative method, Förster resonance energy transfer. Thus, cross-correlation is more effective for studying interactions between membrane-associated proteins in which the labels are on opposite sides of the membrane or are otherwise too spatially separated or misoriented for energy transfer. However, FCS measurements do require a stable target and low-fluorescence background. Thus, assisted by multiphoton microscopy, FCS has begun to become useful in applications to living cell membranes (Schwille et al., 1999).

Using measurements of FcεRI and Lyn diffusion in the membrane, coupled with measurements of association determined by cross-correlation, we are able to simultaneously monitor the time courses for protein–membrane interactions (diffusion) with specific protein–protein interactions (cross-correlation) during IgE signaling on living cells. We find that the association between FcεRI and Lyn is temporally variable and continues long after the initial phosphorylation of the receptor. Lyn exhibits a sustained decrease in lateral diffusion over this same time period. In contrast, a construct consisting of only the membrane-targeting sequence of Lyn labeled with EGFP does not exhibit this diffusion change, nor does full-length Lyn in the presence of a Src family tyrosine kinase inhibitor. The time scale of these protein–protein interactions and diffusion changes suggests that they are subsequent to initial phosphorylation events that occur in ordered lipid environments (Young et al., 2005) and may represent a more mature protein assembly within the membrane that modulates downstream signaling.

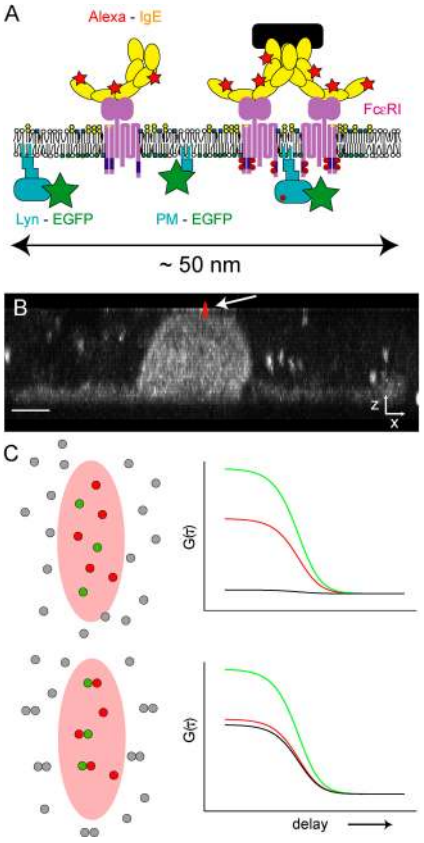

Figure 1. **Observation of fluorescently labeled IgE receptors and Lyn-EGFP kinase on RBL mast cells.** (A) Schematic showing the transmembrane receptor, FcεRI (purple), IgE antibody (yellow) labeled with Alexa Fluor 546 (red stars), Lyn kinase (blue) with EGFP (green stars), a membrane-anchored form of EGFP containing only the myristoylation and palmitoylation sites of Lyn (blue; PM-EGFP), cross-linking antigen (black), and phosphotyrosine sites on Lyn and the receptor (dark red). (B) Side profile of an adherent RBL cell labeled with A^{546}-IgE. The multiphoton excitation volume (arrow) focused on the upper plasma membrane (0.5 × 1.5 μm) is drawn to scale in red. Bar, 5 μm. (C) Dual color cross-correlation FCS observes protein–protein interactions: schematics at left show ellipsoidal focal volume within which fluorescence is excited. Correlation functions ($G(\tau)$) at right are shown for green and red fluorophores and black for the cross-correlation of green with red. The rise of the black cross-correlation curve in the lower example where green and red species are bound together and diffuse together shows that the duration of the interaction exceeds the diffusive dwell time in the focal volume.

Results

For FCS experiments, FcεRI was labeled by Alexa Fluor 488– or Alexa Fluor 546–conjugated IgE (A^{488}-IgE and A^{546}-IgE), which bind irreversibly on the time scale of the measurements (Kulczycki and Metzger, 1974; unpublished data). Lyn was transiently expressed as a chimera with EGFP at its COOH terminus (Lyn-EGFP; Hess et al., 2003) and as a second, membrane-anchored EGFP chimera containing only the NH_2-terminal 10 amino acid sequence of Lyn with a palmitoylation and a myristoylation site, but not the catalytic, SH2, or SH3 domains (PM-EGFP; Pyenta et al., 2003). Because rat basophilic leukemia (RBL) mast cells contain endogenous Lyn kinase, the functional competence of the Lyn-EGFP construct was verified by transiently coexpressing it with a protein tyrosine phosphatase (PTPα) in CHO cells stably expressing FcεRI, as previously described for wild-type Lyn kinase (Young et al., 2005). In this test, antigen-stimulated, Lyn-EGFP–dependent tyrosine phosphorylation of FcεRI was observed (unpublished data), which was consistent with previous results that demonstrated the functional competence of Lyn-EGFP (Kovarova et al., 2001).

Interactions between IgE-FcεRI and Lyn are not readily observable by fluorescence imaging under our conditions of stimulation. Before stimulation with cross-linking antigen (DNP-BSA), both Lyn-EGFP and A^{546}-IgE-FcεRI appear uniformly distributed in the plasma membrane (Fig. 2, A and B). After cross-linking with DNP-BSA for 40 min at 21°C, A^{546}-IgE-FcεRI aggregates into discrete puncta at the cell surface (Fig. 2 D), and these persist and grow for longer time periods,

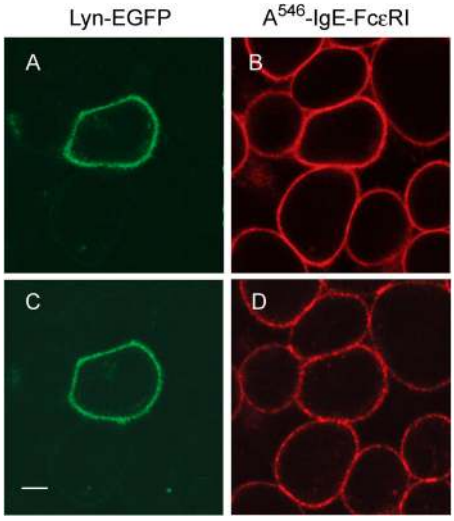

Figure 2. **Spatial distribution of A546-IgE-FcεRI and Lyn-EGFP before and after stimulation with antigen.** (A and B) Multiphoton images showing equatorial distributions of Lyn-EGFP (green; A) and Alexa 546-IgE-FcεRI (red; B) before stimulation with cross-linking antigen. (C and D) Equatorial distributions of Lyn-EGFP (C) and A^{546}-IgE-FcεRI (D) after stimulation with cross-linking antigen for 40 min at 21°C. Bar, 5 μm. Multiphoton excitation wavelength = 860 nm; power = 2.0 mW.

eventually forming large domains if cells are held at 4°C to slow internalization (Thomas et al., 1994). Nevertheless, Lyn-EGFP appeared to remain uniformly distributed at optical resolution during the time of our measurements at 21°C (Fig. 2 C). Thus, coredistribution of Lyn-EGFP accompanying microscopically detectable clustering of IgE receptors is not readily detectable under these conditions, possibly because only a small fraction of the available Lyn-EGFP binds in its competition with the excess coexisting unlabeled Lyn. Furthermore, previous biochemical coimmunoprecipitation studies have suggested that this receptor–kinase interaction is weak and/or transient (Pribluda et al., 1994; Siraganian, 2003). Transient colocalization of Lyn with cross-linked FcεRI has been detected by electron microscopy (Wilson et al., 2000), but real-time kinetics of these interactions have not been observed.

FCS measurements of lateral diffusion

To characterize the lateral mobility of Lyn-EGFP, PM-EGFP, and A^{488}-IgE-FcεRI, we performed FCS measurements before and after IgE receptor cross-linking by multivalent antigen. Intracellular FCS measurements require average fluorophore concentrations that are low enough to make fluctuations distinguishable, yet high enough to differentiate the signal from the background; the optimum is usually ~10–100 molecules in the focal volume, corresponding here to ~100–1,000 per micrometer squared on the membrane. We chose cells with fluorescence levels similar to the images of those in Fig. 2, which correspond to the level that we have empirically found to provide the best signal to noise for multiphoton FCS. In addition, FCS experiments were performed at 21°C to minimize stimulated cell ruffling and spreading, which interfere with these measurements at 37°C, and which may remain as a perturbation at 21°C.

Data from individual cells are shown for each of these proteins in Fig. 3 (A, C, and E). The amplitude curves are normalized to facilitate direct comparison of the diffusion times. For Lyn-EGFP (Fig. 3 A) and A^{488}-IgE–labeled FcεRI (Fig. 3 E) there is an increase in the decay time of the FCS curves from before stimulation (pink) to longer times after 30 min of stimulation by antigen (blue), indicating that both proteins diffuse more slowly through the focal volume and are thus shown to have lower mobility after stimulation. For PM-EGFP (Fig. 3 C), however, there is no detectable shift in the diffusion time as a result of IgE receptor cross-linking with antigen. Fitting each curve requires one or two diffusion coefficients, together with the relative contribution of each. For the inner leaflet–anchored

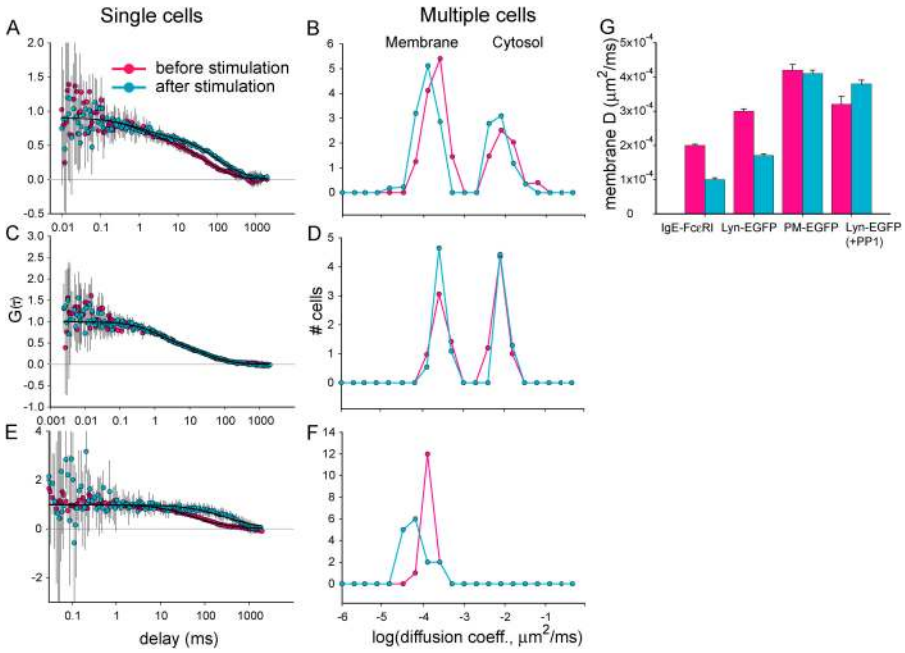

Figure 3. **Diffusion of A^{488}-IgE-FcεRI, Lyn-EGFP, and PM-EGFP before and after stimulation with antigen.** (A, C, and E) FCS autocorrelation curves from single cells: (A) Lyn-EGFP, (C) PM-EGFP, and (E) A^{488}-IgE-FcεRI. The y-axis is the autocorrelation amplitude as a function of delay time (G(τ)), and each curve is the average of five consecutive 10-s measurements, with error bars as measured SD. The after curves are recorded 30 min after stimulation. (B, D, and F) Histograms of diffusion coefficients compiled from multiple cells: (B) Lyn-EGFP (n = 19 cells), (D) PM-EGFP (n = 12 cells), and (F) A^{488}-IgE-FcεRI (n = 15 cells). Bin width = 0.3 μm²/ms. (G) Average membrane-bound diffusion coefficients from the designated peaks in B, D, and F, and for cells in the presence of 20 μM PP1 (n = 11 cells). Error bars are the SEM. Multiphoton excitation wavelength = 905 nm and power = 1.4 mW for all measurements.

proteins Lyn-EGFP and PM-EGFP it is necessary to use a two-component diffusion fit (Larson et al., 2003; Pyenta et al., 2003), whereas for transmembrane FcεRI a one component fit is sufficient both before and after stimulation. It has previously been shown that the diffusibility of individual noncross-linked FcεRI on RBL cells shows diverse diffusive behavior called anomalous subdiffusion, a phenomenon common to cell membrane proteins that is difficult to distinguish from a spread of conventional diffusion coefficients by FCS (Feder et al., 1996).

Diffusion data compiled from multiple cells are shown in Fig. 3 (B, D, and F). For the inner leaflet–anchored proteins, we observe two well resolved diffusion coefficients: one at $D \approx 10^{-4}$ μm^2/ms, corresponding to membrane-associated diffusion, and one at $D \approx 10^{-2}$ μm^2/ms, corresponding to faster diffusion in the cytoplasm (Pyenta et al., 2003). For the IgE receptor, there is a single peak at $D \approx 10^{-4}$ μm^2/ms, corresponding to diffusion in the membrane, and this peak exhibits a significant shift to lower values after cross-linking by antigen, as previously observed by fluorescence photobleaching recovery (Menon et al., 1986). Stimulation by antigen also results in a decrease in the diffusion of the membrane-bound component of Lyn-EGFP and a much smaller, not clearly significant decrease for the cytosolic component (Fig. 3 B). In contrast, there is no stimulated change in the diffusion of PM-EGFP. These distinctive results indicate that the observed decrease in Lyn-EGFP diffusion involves significant protein interactions and is not based solely on compartmentalization provided by ordered membrane lipids ("lipid rafts") that play an important role in regulating the initial phosphorylation of FcεRI by Lyn (Young et al., 2005).

The histograms shown in Fig. 3 are compiled from FCS measurements taken at variable times (5–40 min) after stimulation and from multiple points on the cell surface. The spatial distribution of Lyn does not visibly change during this time, and the bimodal distribution of diffusion coefficients is due primarily to superimposition of the difference between cytosolic and membrane diffusion. For FcεRI, however, the spatial distribution changes considerably during stimulation, and the diffusion coefficient distribution presumably reflects diffusion of the known range of oligomeric states. This heterogeneity is reflected in the width of the distribution after stimulation (Fig. 3 F, blue curve).

As summarized in Fig. 3 G, cross-linking of IgE-FcεRI slows average diffusion of both Lyn-EGFP and labeled IgE-FcεRI in the plasma membrane, whereas the diffusion of PM-EGFP is unchanged. Furthermore, the Src family kinase inhibitor PP1 (Amoui et al., 1997) abolishes the antigen-stimulated decrease in Lyn-EGFP diffusion, suggesting that this change is a consequence of the stimulated tyrosine phosphorylation cascade (Fig. 3 G). In contrast, the cross-link–dependent loss of IgE receptor lateral mobility is independent of stimulated signaling processes, as shown in a previous study (Holowka and Baird, 1996).

FCS cross-correlation measurements of FcεRI–Lyn-EGFP interactions

To investigate whether changes in Lyn-EGFP mobility that result from antigen stimulation are due to interaction between Lyn-EGFP and FcεRI, time-resolved fluorescence cross-correlation was measured between these proteins on live cells. Cross-correlation relies on simultaneous monitoring of the fluorescence from two probes (in this case Alexa Fluor 546 coupled to IgE and EGFP attached to Lyn) as they diffuse through the focal volume. If the two probes diffuse as a single entity, there will be a cross-correlation between their fluorescence fluctuations. The extent of cross-correlation is proportional to the amplitude of the cross-correlation curve, which is the value of the correlation at $\tau = 0$ delay time (e.g., $G(0) \equiv G(\tau)$ at $\tau = 0$). This amplitude has a straightforward interpretation for autocorrelation measurements: the autocorrelation amplitude is the inverse of the average number of molecules in the focal volume (i.e., $G(0) = 0.1$ corresponds to 10 molecules in the focal volume). For cross-correlation measurements, the amplitude of the cross-correlation curve provides a measure of association between the two probes. The fractional association of Lyn-EGFP, F, is proportional to the quotient of the cross-correlation amplitude and the individual autocorrelation amplitude of A^{546}-IgE-FcεRI such that

$$F \propto G_{cross}(0)/G_{Fc\varepsilon RI}(0), \quad (1)$$

where G_{cross} (0) is the amplitude of the cross-correlation and $G_{Fc\varepsilon RI}$ (0) is the amplitude of the A^{546}-IgE-FcεRI autocorrelation. In the simple case of a 1:1 binding stoichiometry and absence of background fluorescence interference, the proportionality relationship can be expressed as equality (Heinze et al., 2000). Because the relationship between A^{546}-IgE-FcεRI fluorescence and Lyn-EGFP fluorescence is likely to be more complicated than a 1:1 ratio, we restrict expression to the proportionality in Eq. 1. This behavior is illustrated in Fig. 4 with autocorrelation curves for Lyn-EGFP (green) and A^{546}-IgE-FcεRI (red) and cross-correlation curves (black) at time points before and after stimulation of a single cell by antigen. Before stimulation, the amplitudes of the Lyn-EGFP and FcεRI autocorrelations are each greater than the cross-correlation amplitude (Fig. 4 A); also note that the FcεRI curve has a slower decay than the Lyn-EGFP curve, as expected for the more slowly diffusing transmembrane receptor. At 6 min after stimulation, the cross-correlation amplitude has increased relative to the amplitudes of the Lyn-EGFP and A^{546}-IgE-FcεRI curves and overlaps the FcεRI curve (Fig. 4 B). At 30 min after stimulation, the cross-correlation amplitude has decreased back to a value similar to that before stimulation (Fig. 4 C), indicating that the fractional association between Lyn-EGFP and the receptor has decreased from the value at 6 min after stimulation. For the example shown in Fig. 4, the number of Lyn-EGFP molecules in the focal volume is less than the number of A^{546}-IgE-FcεRI molecules (the amplitude $G_{Lyn}(0)$ is greater than the amplitude $G_{Fc\varepsilon RI}$ (0)). The overlap between the cross-correlation and the A^{546}-IgE-FcεRI autocorrelation indicates that all the Lyn-EGFP in the focal volume is associated with the labeled receptor and that a fraction of the total labeled receptor is associated with Lyn.

To obtain more detailed information about the time course of association between Lyn-EGFP and the receptor,

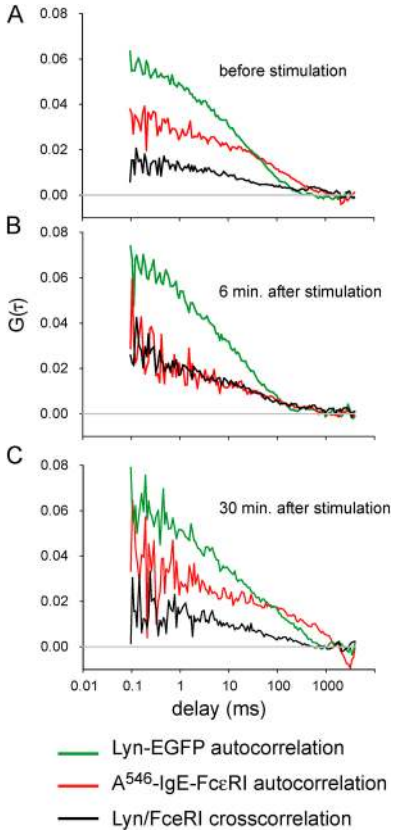

Figure 4. **Fluorescence autocorrelation and cross-correlation curves for A^{546}-IgE-FcεRI and Lyn-EGFP measured on a single cell before and after stimulation with antigen.** (A) Before stimulation; (B) 6 min after stimulation; and (C) 30 min after stimulation. Each curve is the average of five 10-s measurements on a single focal spot. Multiphoton excitation wavelength = 860 nm; power = 1.4 mW.

cross-correlation and individual diffusion measurements were repeated in succession at approximately the same focal spot on the same cell, starting before stimulation and continuing to a time ~30 min after stimulation (see Materials and methods). In this manner, interactions between labeled proteins (association determined from cross-correlation) and between proteins and their microenvironments (diffusion determined from autocorrelation) are obtained in the same time-resolved measurements on individual living cells.

Because the membranes of RBL cells change as the cytoskeleton rearranges and vesicle release begins on the time scale of these experiments, it is particularly likely that after antigenic stimulation the FcεRI aggregates to which Lyn-EGFP binds may move significantly with respect to the stationary FCS focal volumes so that the FCS measurements are possibly sensing areas at slowly variable distances with respect to heterogeneity on the cell surface.

Two such time courses from single cells are shown in Fig. 5 (A and B). Consistent with the steady-state FCS measurements made before and after stimulation (Fig. 3), there is a time-dependent decrease in Lyn-EGFP diffusion after stimulation (Fig. 5, A and B, green curves). The time courses for these diffusion changes are somewhat different for each of the cells shown. As measured by cross-correlation analysis, the amount of Lyn-EGFP associated with IgE-FcεRI increases after stimulation, and these interactions show time-dependent changes that also exhibit somewhat different patterns for each cell (Fig. 5, A and B, black curves). As apparent from these and other data, interactions between Lyn-EGFP and FcεRI are detectable after a variable lag time and appear to undergo rapid, transient variations after an initial increase in association that occurs as the diffusion of Lyn-EGFP is decreasing. These transient interactions occur with varying magnitudes over the ~30 min of observation, whereas Lyn-EGFP diffusion remains persistently reduced after the onset of its stimulation-dependent decrease. By comparison, Lyn-EGFP–FcεRI association in unstimulated cells is consistently low and invariant over the entire measurement period (Fig. 5, A and B, gray curves). Cells that have been monitored in this manner for 30 min at 21°C remain functionally competent, as indicated by their ruffling response to antigen when warmed to 37°C (unpublished data).

When data from seven stimulated cells are averaged, time-dependent increases and decreases in Lyn-EGFP–IgE-FcεRI association are still observed by cross-correlation analysis (Fig. 5 C, black curve). This stimulated association shows an initial peak several hundred seconds after stimulation is initiated and a second larger peak at a longer time. Under these conditions, ~50% of the cells that were monitored show stimulation-dependent increases in IgE-FcεRI–Lyn-EGFP cross-correlation and decreases in Lyn-EGFP diffusion, and this fraction of responding cells is consistent with the percentage of cells showing antiphosphotyrosine-detected responses upon stimulation by patterned lipid bilayers (Wu et al., 2004). Two different types of cross-correlation baseline controls remain low and constant throughout the time course: Lyn-EGFP–IgE-FcεRI in unstimulated cells (Fig. 5 C, gray curve) and PM-EGFP–IgE-FcεRI before and after stimulation (Fig. 5 C, green curve). Consistent with our results for reduction in diffusion, the results of Fig. 5 suggest that the interactions between Lyn-EGFP and IgE-FcεRI that occur several minutes after stimulation may involve structural features of Lyn additional to its membrane-anchoring sequence. In other words, these results suggest that simple association with ordered lipids as expected for PM-EGFP is insufficient to cause the observed interactions with cross-linked FcεRI.

The time course of tyrosine phosphorylation of FcεRI β detected by Western blotting and measured under identical experimental conditions is shown in Fig. 5 C (blue data points and lines). This stimulated phosphorylation is near-maximal ~200 s after stimulation is initiated, which is before the decrease in lateral diffusion of Lyn-EGFP (Fig. 5 D) and the first large burst in cross-correlation (Fig. 5 C), and approximately coincident with the beginning of the decrease in lateral diffusion of Lyn-EGFP (Fig. 5 D), which both begin ~400–500 s after stimulation is initiated. The earliest interactions between Lyn-EGFP and FcεRI during the initiation of ITAM phosphorylation may be too transient or, more likely, involve an insufficient fraction of Lyn-EGFP to be detected above the baseline cross-correlation in these averaged data. However, early interactions detected in some individual cells, such as that in Fig. 5 A, could be relevant to the initiation of receptor phosphorylation by

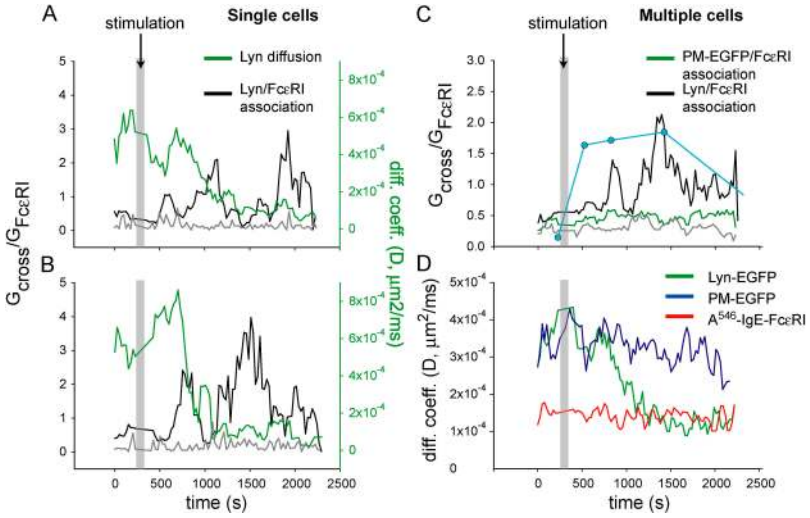

Figure 5. **Time variation of diffusion and cross-correlation for Lyn-EGFP and A^{546}-IgE-FcεRI during stimulation with antigen.** (A and B) Two separate single cell measurements of the time variation of diffusion of Lyn-EGFP (green) and the cross-correlation of Lyn-EGFP with IgE-FcεRI (black). Cross-correlation of Lyn-EGFP with IgE-FcεRI in the absence of stimulation (gray) comes from a separate measurement on a different cell. The y-axis scale on the left side is the ratio of the amplitude of the cross-correlation $G_{cross}(0)$ and the amplitude of the receptor autocorrelation $G_{FcεRI}(0)$, and is proportional to the fraction of Lyn-EGFP associated with the receptor (Eq. 1). The black and gray curves are plotted on this axis. The y-axis on the right side represents diffusion coefficients for Lyn-EGFP. The green curve is plotted on this axis. The gray bar indicates the time of antigen addition. (C) Time-resolved cross-correlation averaged over multiple cells. Black, Lyn-EGFP–IgE-FcεRI in stimulated responding cells (n = 7 cells); green, PM-EGFP–IgE-FcεRI in stimulated cells (n = 6 cells); gray, Lyn-EGFP–IgE-FcεRI in unstimulated cells (n = 3 cells). The blue circles show relative FcεRI β tyrosine phosphorylation, measured by antiphosphotyrosine Western blotting under the same experimental conditions. (D) Time-resolved diffusion averaged over multiple stimulated cells. Green, Lyn-EGFP (n = 7 cells); blue, PM-EGFP (n = 6 cells); red, IgE-FcεRI (n = 13 cells). Multiphoton excitation wavelength = 860 nm; power = 1.4 mW.

Lyn. Other studies have provided biochemical (Pribluda et al., 1994; Field et al., 1997) or ultrastructural (Wilson et al., 2000) evidence for Lyn–FcεRI interactions on a time scale (<200 s) that is relevant to the initiation of FcεRI phosphorylation by Lyn.

Time course for changes in Lyn-EGFP diffusion

Time-resolved diffusion of each labeled protein provides further information about the early events during the signaling process. Whereas Lyn-EGFP shows a substantial decrease in diffusion that begins several hundred seconds after stimulation is initiated (Fig. 5 D, green curve), PM-EGFP shows only a small, perhaps insignificant, change in diffusion (Fig. 5 D, dark blue curve). These diffusion data, when compared with the time-dependent changes in cross-correlation, indicate that the first peak of association occurs during initiation of the change in Lyn-EGFP diffusion, whereas the second, larger, cross-correlation peak occurs after Lyn-EGFP has undergone substantial loss in lateral mobility in the plasma membrane. These results suggest that an interaction with another membrane-associated component, as manifested by the reduction in diffusion, may facilitate the association with FcεRI that is observed because the periodic decreases in cross-correlation do not result in corresponding increases in lateral diffusion. Lateral diffusion of A^{546}-IgE-FcεRI in these measurements is slow and similar to that of Lyn-EGFP after its stimulation-dependent decrease.

Structural basis for IgE receptor–Lyn-EGFP interactions

One possible explanation for the association between Lyn-EGFP and FcεRI detected by cross-correlation is the binding of the SH2 domain of Lyn to the phosphorylated β subunit of FcεRI (Kihara and Siraganian, 1994). To test this, we used a single chain chimeric IgE receptor, αTζ, which has been shown to mediate antigen-stimulated degranulation when cross-linked at 37°C, but which does not associate with FcεRI β or mediate its phosphorylation after stimulation (Gosse et al., 2005). Average values for associations of Lyn-EGFP with FcεRI and with αTζ before and after cell stimulation, as detected by cross-correlation, are summarized in Fig. 6. For these comparisons, inhibition of actin polymerization by cytochalasin D was necessary for FCS measurements with αTζ to prevent αTζ internalization, which occurs more rapidly after antigen cross-linking than does FcεRI internalization (unpublished data). As shown in Fig. 6, the stimulated interaction between Lyn-EGFP and FcεRI exhibits partial sensitivity to cytochalasin D, suggesting some role for the actin cytoskeleton in mediating this association. In the presence of cytochalasin D, the stimulated increase in cross-correlation between Lyn-EGFP and αTζ is similar to that for Lyn-EGFP and FcεRI. Cross-correlation between PM-EGFP and FcεRI does not increase significantly due to stimulation, as also seen in Fig. 5. Thus, these results indicate that the stimulated association of Lyn-GFP with IgE receptors detected by FCS cross-correlation is sensitive to inhibition of actin polymerization, but is independent of interactions between Lyn-EGFP and FcεRI β.

Discussion

Using FCS we have demonstrated that it is possible to observe the stimulated interaction between two labeled proteins—A^{546}-IgE-FcεRI and Lyn-EGFP—while also observing the lateral diffusion of these proteins in the plasma membrane of live cells. In this study, measurement of real-time changes in the lateral diffusion of Lyn-EGFP indicates that antigen stimulates a time-dependent interaction of this kinase with a plasma membrane–associated component that diffuses more slowly than Lyn-EGFP itself. Changes in Lyn diffusion due to FcεRI activation have not previously been reported, and the interactions that these diffusion changes detect are initiated with a variable lag time, beginning on average >400 s after antigen addition at 21°C (Fig. 5 D). This change in Lyn mobility first appears >200 s after stimulated FcεRI tyrosine phosphorylation reaches a near-maximal value, suggesting that it reflects an in-

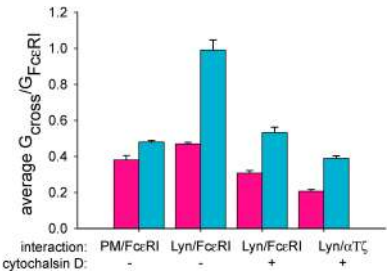

Figure 6. **Average cross-correlation values before and after stimulation by antigen.** Cells were stimulated by antigen in the absence or presence of 1 μM cytochalasin D. Error bars represent the SEM for PM-EGFP–FcεRI ($n = 3$), Lyn-EGFP–FcεRI ($n = 7$), Lyn-EGFP–FcεRI with cytochalasin D ($n = 4$), and Lyn-EGFP–chimeric αTζ with cytochalasin D ($n = 7$).

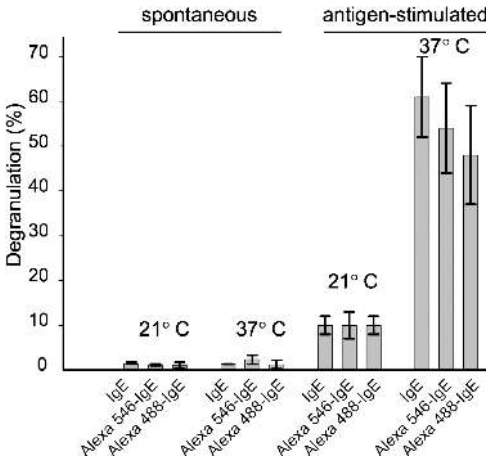

Figure 7. **Degranulation responses for RBL mast cells sensitized with various IgEs and stimulated at 21 or 37°C.** Cells were sensitized with IgE derivatives as described in Materials and methods and stimulated with 1 μg/ml DNP-BSA for 1 h at 21 or at 37°C. Release of β-hexosaminidase into cell supernatants was measured as described in Materials and methods. Error bars represent the SD from three separate experiments.

teraction downstream of FcεRI signal initiation. Interactions between cross-linked IgE-FcεRI and Lyn-EGFP detected by cross-correlation are also observed to occur with a similar delay in onset, which is consistent with a direct relationship between these processes. This coordinated change is most evident in the data from individual cells (Fig. 5, A and B), but it remains in the averaged time courses as well, in spite of substantial cell–cell variation (Fig. 5, C and D). All of these results indicate that the interactions detected are a consequence of signal initiation, rather than a requirement for such.

A surprising discovery of this study is the temporally variable association between Lyn-EGFP and IgE-FcεRI detected by cross-correlation FCS. The time-dependent changes observed are most dramatic in the time courses of individual cells, and this variation could be caused, in principle, by clusters of cross-linked receptors moving in and out of the focal volume. However, we see no indication of this from analysis of the time courses of A^{546}-IgE fluorescence intensity across this time scale.

On the time scale of these fluctuations, several other oscillatory processes occur. Previous measurements showed oscillatory Ca^{2+} responses after stimulation at 37°C with comparable time scales (Millard et al., 1989). Recently, we have seen Ca^{2+} oscillations after stimulation at 21–25°C that are similarly fast and comparable to the cross-correlation fluctuation time scales (unpublished data). The biochemical basis for stimulated oscillations in intracellular Ca^{2+} in RBL mast cells is not fully understood (Millard et al., 1989; Meyer and Stryer, 1991), and it is possible that periodic interactions between Lyn and FcεRI could couple to such oscillations. Note that Lyn expression is necessary for normal Ca^{2+} responses in bone marrow–derived mast cells, even though Fyn kinase is sufficient for other signaling pathways activated in these cells (Parravicini et al., 2002).

An alternative explanation for temporally variable cross-correlation FCS is cytoskeletally driven membrane perturbations that have previously been observed in RBL cells freshly plated after culture. Thus, cell membrane motions could be responsible for at least some of the oscillatory behavior shown in Fig. 6. It has not yet been possible to control for this possible artifact, but new nanoscopic strategies similar to the patterned bilayer experiments of Wu et al. (2004) or waveguide substrate structures (Levene et al., 2003) may be able to resolve this issue in the next several years.

Although the association between Lyn and FcεRI is temporally variable, there is a persistent decrease in Lyn diffusion during signaling. A decrease in lateral mobility for Lck tyrosine kinase has been observed by single molecule imaging of T cells (Ike et al., 2003). Furthermore, this group observed a localized decrease in Lck diffusion in the vicinity of cross-linked receptors, which is consistent with the interactions we observe between Lyn and FcεRI by cross-correlation analysis. These cumulative results suggest that such behavior might be a more general feature of Src family kinases during immune cell signaling. The sustained decrease in lateral diffusion that accompanies time-dependent variations in the interactions between IgE-FcεRI and Lyn-EGFP suggests that Lyn-EGFP may bind to other membrane-associated components, and this may facilitate the interaction of Lyn with cross-linked FcεRI. The structural basis for these interactions is not yet clear, but because of the absence of these interactions with PM-EGFP they are likely to require a protein domain of Lyn, in addition to its NH_2-terminal membrane-anchoring sequence. Although association with ordered lipid rafts is clearly insufficient for the interactions that result in the loss of Lyn-EGFP lateral mobility, interactions with proteins that associate with lipid compartments, such as Cpb/PAG (Ohtake et al., 2002) or flotillins (Rajendran et al., 2003), could contribute to the experimental results. A previous study indicated that the SH2 domain of Lyn is necessary for the activation of Syk kinase and consequent downstream signaling, but not for stimulated receptor phosphorylation (Honda et al., 2000). Other studies indicated that interactions mediated by the SH3 domain of Lyn (Stauffer et al., 1997) or the T cell–specific Src kinase Lck (Denny et al., 1999) are important for downstream signaling by FcεRI and T cell receptors, respectively.

Lyn has also been shown to play negative roles in regulating Fyn kinase, phosphoinositide 3-kinase, and degranulation (Parravicini et al., 2002; Odom et al., 2004), and the interactions that we detect may also be relevant to this function of Lyn. In $Lyn^{-/-}$ mast cells, stimulated tyrosine phosphorylation of

FcεRI and other proteins is more sustained, albeit reduced in magnitude (Hernandez-Hansen et al., 2004), so it is possible that the interaction between Lyn and FcεRI that we detect is important for regulating the time course of the tyrosine phosphorylation response. Consistent with this idea, cytochalasin D reduces the magnitude of this stimulated interaction (Fig. 7) while facilitating a more sustained phosphorylation response to antigen (Holowka et al., 2000). Although ordered membrane lipids may play a role in facilitating the interactions detected, the targeting of EGFP by the PM sequence is clearly not sufficient for these interactions to occur.

Studies using chemical cross-linking in permeabilized RBL cells to stabilize stimulated interactions showed that Lyn can be coisolated with cross-linked FcεRI in a kinase-dependent manner (Yamashita et al., 1994). Under these conditions of stabilization, a large number of other proteins were also coisolated with FcεRI, both before and after stimulation (Mao et al., 1995). In these studies and the present experiments it is not yet clear whether the interactions detected between Lyn and FcεRI (or αTζ) are direct, or whether other unidentified components are mediating these interactions. A recent study using patterned lipid bilayers as localized sites for FcεRI-mediated stimulation found that Lyn-EGFP accumulates at these sites more slowly than the activation of tyrosine phosphorylation there, but more rapidly than PM-EGFP (Wu et al., 2004). In that situation, the accumulation of Lyn-EGFP at the micrometer-sized lipid bilayer patches was inhibited by cytochalasin D, suggesting a strong dependence on actin polymerization for the interactions observed. The partial sensitivity to cytochalasin D for the interaction detected by FCS cross-correlation shown in Fig. 6 indicates that the actin cytoskeleton plays a significant role in mediating this interaction as well and suggests that it may be related to the interaction detected using patterned bilayers. Association between the chimeric receptor for IgE and Lyn-EGFP detected by cross-correlation indicates that this interaction is not mediated by the β subunit of FcεRI, and, thus, this interaction is not relevant to the role of FcεRI β in amplification of the stimulated tyrosine phosphorylation response (Kraft et al., 2004).

In summary, our results show that antigen cross-linking of IgE-FcεRI complexes stimulates a time-dependent decrease in the lateral diffusion of Lyn kinase and a temporally coincident onset of Lyn–FcεRI association that follows in time and is the consequence of stimulated tyrosine phosphorylation. Comparison of the temporal variations in these Lyn–FcεRI interactions to the persistent decrease in Lyn diffusion suggests a process that involves additional cellular components and is relevant to the regulation of downstream signaling events such as Ca^{2+} mobilization and degranulation. These results demonstrate the capacity of cross-correlation fluorescence spectroscopy to provide new insights into the dynamics of receptor-mediated signaling processes in living cells.

The authors must point out that this research does not address the quandary associated with the usual concept of lipid rafts. It does appear consistent with the idea that understanding of the concept of lipid rafts must take into account lipid phases and their phase transitions, including the possibility of continuous phase transition following established statistical thermodynamics in two-dimensional systems (Baumgart et al., 2003, 2005). But this is surely not sufficient for understanding cellular plasma membranes.

Discussions of lipid rafts frequently take the viewpoint that heterogeneity of protein distribution is attributable entirely to their segregation into certain preferred lipid phases. This oversimplification overlooks the fundamental reciprocal interaction between solvent and solutes in any solution where all constituents contribute to the negative free energy of mixing that establishes solution equilibrium. One must recognize the thermodynamic participation of the proteins that have repeatedly been demonstrated to occupy about one third of eukaryotic cell plasma membranes. Experiments illustrating this showed that the unselected proteins on RBL cells actually obey the statistical thermodynamics of the Langmuir absorption isotherm, which takes into account the consumption of available space occupied by the protein molecules on the cell surface (Ryan et al., 1988).

Previous observations of an effect of microscopic IgE receptor clusters on the closely surrounding lipid matrix are relevant to the results reported here but unfortunately do not allow deeper interpretation of rafts. However, Thomas et al. (1994) and Pyenta et al. (2003) did show, through the use of localized fluorescence measurements, that certain lipids and lipid-like dyes tended to aggregate at the microscopic clusters of antigen cross-linked IgE receptors and to be locally restrained within ∼1 μm with retarded diffusive exchange. That kind of inverse interaction is generally ignored in lipid raft discussions. In the raft discussion here, the interactions with the cellular cytoskeleton and the dynamics of lipid endo- and exocytosis are omitted for simplicity. Neglect of the inverse interaction is unfortunately common in more general lipid raft studies. We are currently studying that issue in related RBL cell model systems, but any comment at this point would be premature. We can only say that the simplistic concepts associated with the term lipid rafts have stimulated both chaotic error and careful scientific study and that they were not the subject of this study. Unfortunately, definitive comprehension of plasma membrane dynamics is elusive.

Materials and methods

Reagents

An affinity-purified goat polyclonal antibody to human IgE (huIgE) was obtained from MP Biomedicals. Mouse monoclonal antiphosphotyrosine (clone 4G10) was obtained from Upstate Biotechnology. The B isoforms of Lyn-EGFP (Hess et al., 2003) and PM-EGFP (Pyenta et al., 2001) vectors were constructed as described previously. BSA was conjugated with an average of 15 DNP groups (DNP-BSA, multivalent antigen; Posner et al., 1992). PP1 was purchased from BIOMOL Research Laboratories, Inc.

Mouse monoclonal DNP-specific IgE (moIgE) was purified as described previously (Posner et al., 1992). Purified myeloma huIgE PS was either obtained from Cortex Biochem Inc. or a gift from C. Torigoe (National Institutes of Health, Bethesda, MD). IgE in pH 8.5 borate-buffered saline (200 mM boric acid, 33 mM NaOH, and 160 mM NaCl) was fluorescently labeled using Alexa Fluor 546 or 488 dye kits at the recommended dye/protein ratios (Invitrogen) for 45 min for Alexa Fluor 546 or 2 h for Alexa Fluor 488 at 21°C with stirring in the dark. Reaction mixtures were dialyzed extensively in PBS with EDTA (0.15 M NaCl, 10 mM sodium phosphate, and 1 mM EDTA, pH 7.4) at 4°C. Fluorescent IgEs thus modified had ∼7–8 dye molecules per IgE. To evaluate the functional capacity of A^{488}-IgE and A^{546}-IgE, antigen-stimulated degranulation was performed with RBL-2H3 cells sensitized by these modified IgEs; both were found to mediate responses equivalent to unmodified IgE, at 21 and 37°C, as shown in Fig. 7.

Cells and stimulation

Monolayer cultures of RBL-2H3 cells (Barsumian et al., 1981) were maintained in MEM supplemented with 20% FBS (Atlanta Biologicals, Inc.) and 10 μg/ml of gentamicin sulfate. All cell culture materials were obtained from GIBCO BRL, unless otherwise noted.

Lyn-EGFP or PM-EGFP were transiently transfected into RBL cells, some of which were clones stably transfected with the chimeric IgE receptor αTζ and maintained in G418 media (Gosse et al., 2005) using the Geneporter transfection reagent (Gene Therapy Systems) in Opti-MEM I Reduced Serum Medium (Invitrogen). Cells at ~50% confluency in 35-mm wells (MatTek) were transfected with 1 μg of either Lyn-EGFP or PM-EGFP diluted with 1 μg pCDNA3 empty vector to optimize the ratio of EGFP to A^{546}-IgE fluorescence for FCS experiments with minimal bleed-through. Cells were incubated with the DNA–Geneporter complexes for 1 h at 37°C, and 0.1 μM phorbol 12,13-dibutyrate (Sigma-Aldrich) in Opti-MEM I was added to promote fluid phase phagocytosis and DNA uptake. After an additional 4–6 h at 37°C, the cells were washed thoroughly to remove the phorbol 12,13-dibutyrate and cultured overnight in fresh RBL media. Experiments were performed ~24 h after transfection.

Immediately before experiments, IgE receptors were labeled with A^{546}-IgE or A^{488}-IgE at 21°C. MatTek wells containing transfected cells were washed and incubated with 10 μg/ml A^{546}-moIgE or A^{488}-moIgE for FcεRI, or 30 μg/ml A^{546}-huIgE for αTζ in buffered saline solution (BSS; 135 mM NaCl, 5 mM KCl, 1.8 mM $CaCl_2$, 1 mM $MgCl_2$, 5.6 mM glucose, 20 mM Hepes, and 1 mg/ml BSA, pH 7.4) for 20 min. Cells were washed and measured in BSS in the absence or presence of 20 μM PP1 (Lyn kinase inhibitor) or 1 μM cytochalasin. For stimulation, A^{488}- or A^{546}-moIgE-FcεRI was cross-linked with 1 μg/ml DNP-BSA and A^{546}-huIgE-αTζ was cross-linked with 10 μg/ml anti-huIgE in BSS at 21°C.

FCS

FCS measurements and multiphoton images were acquired on a home-built two-photon FCS microscope, as previously described (Larson et al., 2003). In brief, a tunable, mode-locked Ti:sapphire laser (model Tsunami; Spectra-Physics) was operated at 80 MHz with 200-fs pulses. The beam was raster scanned and positioned at the sample with a confocal scan box (model MRC 600; Bio-Rad Laboratories). Excitation and emission were focused through a 63× 1.2 NA water immersion C-apochromat (Carl Zeiss MicroImaging, Inc.). The same detectors (GaAsP photomultipliers; Hamamatsu) were used for both imaging and FCS. Excitation wavelength and laser power are noted in the figure legends. All measurements were made at 21°C.

For FCS measurements of lateral diffusion before and after stimulation, multiple cells from the same dish were measured taking the average of five 10-s measurements from each focal spot. For time-resolved measurements, a baseline was collected at a single spot on top of the cell, antigen was added, and measurements were resumed after 30–60 s. Autocorrelation measurements were alternated with cross-correlation measurements for 170 10-s measurements on the same cell at the same point (85 cross-correlations alternating with 85 autocorrelations). Thus, the effective time resolution of the cross-correlation or diffusion data points in a time course is 20 s. Cells were selected for measurements based on appropriate fluorescence intensities of the labels (EGFP or Alexa dyes) for high quality FCS data.

The FCS correlation curves were analyzed in a manner similar to that previously described (Larson et al., 2003). Auto-correlation curves were fit to two diffusion coefficients in the case of Lyn-GFP and PM-GFP and one diffusion coefficient in the case of IgE-FcεRI. Dimensions of the two-photon FCS volume are determined from a priori knowledge of the focal volume (Larson, 2003). Cross-correlation curves were fit with two diffusion coefficients and the amplitude $G_{cross}(0)$ was extracted from the fit. The ratio of autocorrelation amplitude to cross-correlation amplitude (Eq. 1, *F*) was calculated from the cross-correlation and the autocorrelation measured immediately before. Data analysis of time-resolved FCS measurements was done with an automated fitting routine written using Interactive Data language software (Research Systems, Inc.).

Functional assays

As previously described (Naal et al., 2004), degranulation was determined using the standard β-hexosaminidase assay. RBL cells attached to microtiter wells were sensitized with A^{546}-IgE, A^{488}-IgE, or unlabeled IgE immediately before the experiment (as in Cells and stimulation) and stimulation at either 21 or 37°C was performed with 1 μg/ml DNP-BSA for 1 h.

For measurement of stimulated tyrosine phosphorylation, attached RBL cells sensitized with A^{546}-IgE (as in Cells and stimulation) were incubated with or without 1 μg/ml DNP-BSA for various times at 21°C and boiled in SDS sample buffer containing 2% β-mercaptoethanol. On 12% SDS-PAGE gels, 8,000 cell equivalents were loaded per lane, and antiphosphotyrosine immunoblotting was performed as previously described (Young et al., 2005). Phosphorylated FcεRI β bands were quantified with UN-SCAN-IT software (Scientific Software Service) and plotted as relative levels of FcεRI β phosphorylation.

Additional editorial assistance was provided by Mark A. Williams at Cornell University (W.W. Webb's laboratory).

This research was supported by National Institutes of Health (NIH) grant AI18306, NIH-National Institute of Biomedical Imaging and Bioengineering grant 9 P41 EB001976 for the Developmental Resource for Biophysical Imaging Opto-Electronics, and National Science Foundation grant DBI-0080792. J.A. Gosse was supported by the W.M. Keck Foundation Program in Biophysics of Signal Transduction at Cornell University. D.R. Larson was supported by the Nanobiotechnology Center at Cornell University (ECS-9876771).

Submitted: 22 March 2005
Accepted: 14 September 2005

References

Amoui, M., P. Draber, and L. Draberova. 1997. Src family-selective tyrosine kinase inhibitor, PPI, inhibits both FcεRI- and Thy-1-mediated activation of rat basophilic leukemia cells. *Eur. J. Immunol.* 27:1881–1886.

Barsumian, E.L., C. Isersky, M.G. Petrin, and R. Siraganian. 1981. IgE-induced histamine release from rat basophilic leukemia cell lines: isolation of releasing and nonreleasing clones. *Eur. J. Immunol.* 11:317–323.

Baumgart, T., S.T. Hess, and W.W. Webb. 2003. Imaging coexisting fluid domains in biomembrane models coupling curvature and line tension. *Nature.* 425:821–824.

Baumgart, T., S. Das, W.W. Webb, and J.T. Jenkins. 2005. Membrane elasticity in giant vesicles with fluid phase coexistence. *Biophys. J.* 89:1067–1080.

Blank, U., C. Ra, L. Miller, K. White, H. Metzger, and J.P. Kinet. 1989. Complete structure and expression in transfected cells of high affinity IgE receptor. *Nature.* 337:187–189.

Denk, W., J.H. Strickler, and W.W. Webb. 1990. Two-photon laser scanning fluorescence microscopy. *Science.* 248:73–76.

Denny, M.F., H.C. Kaufman, A.C. Chan, and D.B. Straus. 1999. The Lck SH3 domain is required for activation of the mitogen-activated protein kinase pathway but not the initiation of T-cell antigen receptor signaling. *J. Biol. Chem.* 274:5146–5152.

Feder, T.J., I. Brust-Mascher, J.P. Slattery, B. Baird, and W.W. Webb. 1996. Constrained diffusion or immobile fraction on cell surfaces: a new interpretation. *Biophys. J.* 70:2767–2773.

Field, K.A., D. Holowka, and B. Baird. 1997. Compartmentalized activation of the high affinity immunoglobulin E receptor within membrane domains. *J. Biol. Chem.* 272:4276–4280.

Gosse, J.A., A. Wagendnecht-Wiesner, D. Holowka, and B. Baird. 2005. Transmembrane sequences are determinants of immunoreceptor signaling. *J. Immunol.* 175:2123–2131

Heinze, K.G., A. Koltermann, and P. Schwille. 2000. Simultaneous two-photon excitation of distinct labels for dual-color fluorescence crosscorrelation analysis. *Proc. Natl. Acad. Sci. USA.* 97:10377–10382.

Hernandez-Hansen, V., A.J. Smith, Z. Surviladze, A. Chigaev, T. Mazel, J. Kalesnikoff, C.A. Lowell, G. Krystal, L.A. Sklar, B.S. Wilson, and J.M. Oliver. 2004. Dysregulated FcepsilonRI signaling and altered Fyn and SHIP activities in Lyn-deficient mast cells. *J. Immunol.* 173:100–112.

Hess, S.T., E.D. Sheets, A. Wagenknecht-Wiesner, and A.A. Heikal. 2003. Quantitative analysis of the fluorescence properties of intrinsically fluorescent proteins in living cells. *Biophys. J.* 85:2566–2580.

Holowka, D., and B. Baird. 1996. Antigen-mediated IgE receptor aggregation and signaling: a window on cell surface structure and dynamics. *Annu. Rev. Biophys. Biomol. Struct.* 25:79–112.

Holowka, D., E.D. Sheets, and B. Baird. 2000. Interactions between Fc(epsilon)RI and lipid raft components are regulated by the actin cytoskeleton. *J. Cell Sci.* 113:1009–1019.

Holowka, D., J.A. Gosse, A.T. Hammond, X. Han, P. Sengupta, N.L. Smith, A. Wagendnecht-Wiesner, M. Wu, R.M. Young, and B. Baird. 2005. Lipid segregation and IgE receptor signaling: a decade of progress. *Biochim. Biophys. Acta.* 10.1016/j.bbamcr.2005.06.007.

Honda, Z.-i., T. Suzuki, H. Kono, M. Okada, T. Yamamoto, C. Ra, Y. Morita, and K. Yamamoto. 2000. Sequential requirements of the N-terminal palmitoylation site and SH2 domain of Src family kinases in the initiation and progression of Fcvarepsilon RI signaling. *Mol. Cell. Biol.* 20:1759–1771.

Ike, H., A. Kosugi, A. Kato, R. Iino, H. Hirano, T. Fujiwara, K. Ritchie, and A. Kusumi. 2003. Mechanism of Lck recruitment to the T-cell receptor cluster as studied by single-molecule-fluorescence video imaging. *ChemPhysChem.* 4:620–626.

Kihara, H., and R. Siraganian. 1994. Src homology 2 domains of Syk and Lyn bind to tyrosine-phosphorylated subunits of the high affinity IgE receptor. *J. Biol. Chem.* 269:22427–22432.

Kinet, J.-P. 1999. The high-affinity IgE receptor (Fc epsilon RI): from physiology to pathology. *Annu. Rev. Immunol.* 17:931–972.

Kovarova, M., P. Tolar, R. Arudchandran, L. Draberova, J. Rivera, and P. Draber. 2001. Structure-function analysis of Lyn kinase association with lipid rafts and initiation of early signaling events after Fcvarepsilon receptor I aggregation. *Mol. Cell. Biol.* 21:8318–8328.

Kraft, S., S. Rana, M.H. Jouvin, and J.P. Kinet. 2004. The role of the FcepsilonRI beta-chain in allergic diseases. *Int. Arch. Allergy Immunol.* 135:62–72.

Kulczycki, A., and H. Metzger. 1974. The interaction of IgE with rat basophilic leukemia cells. II. Quantitative aspects of the binding reaction. *J. Exp. Med.* 140:1676–1695.

Larson, D.R. 2003. Optical approaches to the study of nanoparticles and biology: quantum dots, silica dots, and retroviruses. Ph.D. thesis. Cornell University, Ithaca, NY. 155 pp.

Larson, D.R., Y.M. Ma, V.M. Vogt, and W.W. Webb. 2003. Direct measurement of Gag–Gag interaction during retrovirus assembly with FRET and fluorescence correlation spectroscopy. *J. Cell Biol.* 162:1233–1244.

Levene, M.J., J. Korlach, S.W. Turner, M. Foquet, H.G. Craighead, and W.W. Webb. 2003. Zero-mode waveguides for single molecule analysis at high concentrations. *Science.* 299:682–686.

Magde, D., E. Elson, and W.W. Webb. 1972. Thermodynamic fluctuations in a reacting system. Measurement by fluorescence correlation spectroscopy. *Phys. Rev. Lett.* 29:705–708.

Mao, S.Y., T. Yamashita, and H. Metzger. 1995. Chemical cross-linking of IgE-receptor complexes in RBL-2H3 cells. *Biochemistry.* 34:11968–11977.

Menon, A.K., D. Holowka, W.W. Webb, and B. Baird. 1986. Cross-linking of receptor-bound Ige to aggregates larger than dimers leads to rapid immobilization. *J. Cell Biol.* 102:541–550.

Meyer, T., and L. Stryer. 1991. Calcium spiking. *Annu. Rev. Biophys. Biophys. Chem.* 20:153–174.

Millard, P.J., T.A. Ryan, W.W. Webb, and C. Fewtrell. 1989. Immunoglobulin E receptor cross-linking induces oscillations in intracellular free ionized calcium in individual tumor mast cells. *J. Biol. Chem.* 264:19730–19739.

Naal, R.M.Z.G., J. Tabb, D. Holowka, and B. Baird. 2004. In situ measurement of degranulation as a biosensor based on RBL-2H3 mast cells. *Biosens. Bioelectron.* 20:791–796.

Odom, S., G. Gomez, M. Kovarova, Y. Furumoto, J.J. Ryan, H.V. Wright, C. Gonzalez-Espinosa, M.L. Hibbs, K.W. Harder, and J. Rivera. 2004. Negative regulation of immunoglobulin E–dependent allergic responses by Lyn kinase. *J. Exp. Med.* 199:1491–1502.

Ohtake, H., N. Ichikawa, M. Okada, and T. Yamashita. 2002. Cutting edge: transmembrane phosphoprotein Csk-binding protein/phosphoprotein associated with glycosphingolipid-enriched microdomains as a negative feedback regulator of mast cell signaling through the FcepsilonRI. *J. Immunol.* 168:2087–2090.

Parravicini, V., M. Gadina, M. Kovarova, S. Odom, C. Gonzalez-Espinosa, Y. Furumoto, S. Saitoh, L.E. Samelson, J.J. O'Shea, and J. Rivera. 2002. Fyn kinase initiates complementary signals required for IgE-dependent mast cell degranulation. *Nat. Immunol.* 3:741–748.

Posner, R.G., B. Lee, D.H. Conrad, D. Holowka, B. Baird, and B. Goldstein. 1992. Aggregation of IgE-receptor complexes on rat basophilic leukemia cells does not change the intrinsic affinity but can alter the kinetics of the ligand-IgE interaction. *Biochemistry.* 31:5350–5356.

Pribluda, V.S., C. Pribluda, and H. Metzger. 1994. Transphosphorylation as the mechanism by which the high-affinity receptor for IgE is phosphorylated upon aggregation. *Proc. Natl. Acad. Sci. USA.* 91:11246–11250.

Pyenta, P.S., D. Holowka, and B. Baird. 2001. Cross-correlation analysis of inner-leaflet-anchored green fluorescent protein co-redistributed with IgE receptors and outer leaflet lipid raft components. *Biophys. J.* 80:2120–2132.

Pyenta, P.S., P. Schwille, W.W. Webb, D. Holowka, and B.A. Baird. 2003. Lateral diffusion of membrane lipid-anchored probes before and after aggregation of cell surface IgE-receptors. *J. Phys. Chem. A.* 107:8310–8318.

Rajendran, L., M. Masilamani, S. Solomon, R. Tikkanen, C.A. Stuermer, H. Plattner, and H. Illges. 2003. Asymmetric localization of flotillins/reggies in preassembled platforms confers inherent polarity to hematopoietic cells. *Proc. Natl. Acad. Sci. USA.* 100:8241–8246.

Rivera, J., J.R. Cordero, Y. Furumoto, C. Luciano-Montalvo, C. Gonzalez-Espinosa, M. Kovarova, S. Odom, and V. Parravicini. 2002. Macromolecular protein signaling complexes and mast cell responses: a view of the organization of IgE-dependent mast cell signaling. *Mol. Immunol.* 38: 1253–1258.

Ryan, T.A., J. Myers, D. Holowka, B. Baird, and W.W. Webb. 1988. Molecular crowding on the cell-surface. *Science.* 239:61–64.

Schwille, P., U. Haupts, S. Maiti, and W.W. Webb. 1999. Molecular dynamics in living cells observed by fluorescence correlation spectroscopy with one- and two-photon excitation. *Biophys. J.* 77:2251–2265.

Siraganian, R.P. 2003. Mast cell signal transduction from the high-affinity IgE receptor. *Curr. Opin. Immunol.* 15:639–646.

Stauffer, T.P., C.H. Martenson, J.E. Rider, B.K. Kay, and T. Meyer. 1997. Inhibition of Lyn function in mast cell activation by SH3 domain binding peptides. *Biochemistry.* 36:9388–9394.

Thomas, J.L., D. Holowka, B. Baird, and W.W. Webb. 1994. Large-scale coaggregation of fluorescent lipid probes with cell-surface proteins. *J. Cell Biol.* 125:795–802.

Webb, W.W. 2001. Fluorescence correlation spectroscopy: inception, biophysical experimentations and prospectus. *Appl. Opt.* 40:3969–3983.

Wilson, B.S., J.R. Pfeiffer, and J.M. Oliver. 2000. Observing FcεRI signaling from the inside of the mast cell membrane. *J. Cell Biol.* 149:1131–1142.

Wu, M., D. Holowka, H.G. Craighead, and B. Baird. 2004. Visualization of plasma membrane compartmentalization with patterned lipid bilayers. *Proc. Natl. Acad. Sci. USA.* 101:13798–13803.

Xu, Y., K.W. Harder, N.D. Huntington, M.L. Hibbs, and D.M. Tarlinton. 2005. Lyn tyrosine kinase: accentuating the positive and the negative. *Immunity.* 22:9–18.

Yamashita, T., S. Mao, and H. Metzger. 1994. Aggregation of the high-affinity IgE receptor and enhanced activity of p53/ 56lyn protein-tyrosine kinase. *Proc. Natl. Acad. Sci. USA.* 91:11251–11255.

Young, R.M., X.M. Zheng, D. Holowka, and B. Baird. 2005. Reconstitution of regulated phosphorylation of Fc epsilon RI by a lipid raft-excluded protein-tyrosine phosphatase. *J. Biol. Chem.* 280:1230–1235.